

pH regulation in acid-stressed leaves of pea plants grown in the presence of nitrate or ammonium salts: studies involving ^{31}P -NMR spectroscopy and chlorophyll fluorescence

Richard Bligny ^a, Elisabeth Gout ^a, Werner Kaiser ^b, Ulrich Heber ^{b,*}, David Walker ^c,
Roland Douce ^a

^a *Laboratoire de Physiologie Cellulaire Végétale, DBMS, Centre d'Etudes Nucléaires de Grenoble and Université Joseph Fourier, 38054 Grenoble, France*

^b *Julius von Sachs Institute, University of Würzburg, 97084 Würzburg, Germany*

^c *Ecological Research Station Biddlstone, University of Sheffield, Sheffield, S10 2TN, England*

Received 31 December 1996; accepted 24 January 1997

Abstract

^{31}P nuclear magnetic resonance spectroscopy was used to monitor changes of cytoplasmic and vacuolar pH values in leaf tissues from young pea plants which had been grown in hydroponic culture with either nitrate or ammonium salts as sources of nitrogen. When acid stress was applied by the addition of 15% CO_2 to air (5.1 mM CO_2 in solution), cytoplasmic pH values decreased fast by 0.5 pH units and then increased slowly without reaching the initial pH, while vacuolar pH values decreased by 0.1 pH units. Under anaerobic conditions, the cytoplasmic pH decreased by one pH unit and the vacuolar pH increased by almost 0.4 pH units. These changes were rapidly reversed when CO_2 was removed from air or, after anaerobiosis, by aeration. However, with mannose present during and after anaerobiosis, aeration failed to bring pH values back to the levels observed before anaerobiosis. Simultaneously, mannose phosphates accumulated and cytoplasmic phosphate disappeared. Since loss of phosphate decreases ATP levels, the observations suggest that ATP-dependent pumping of protons into the vacuole restored the cytoplasmic pH partially during acidification by CO_2 and fully after anaerobiosis. Photosynthesis was initially inhibited by high CO_2 and then restored indicating that protons are exported not only across the tonoplast into the vacuole but also across the chloroplast envelope into the cytosol. No large differences in pH regulation were observed in leaves of pea plants which were grown with either nitrate or ammonium salts. Apparently, retarded growth of ammonium-fertilized plants cannot be attributed to ineffective pH regulation.

Keywords: Acid stress; Anaerobiosis; NMR analysis; pH regulation; Photosynthesis; Ion transport; Tonoplast ATPase

1. Introduction

Acid stress is a condition suffered by plants under different conditions. Excess of acid may decrease the

pH of the normally slightly alkaline cytoplasm of plant cells under glycolysis or by leakage of acids from the vacuoles when flooding deprives plants of oxygen. Acid may also be introduced from outside. Leaves are effective gas exchange systems. Air pollutants such as sulfur dioxide or nitrogen dioxide enter

* Corresponding author. Fax: +49 931 8886158.

leaves through open stomata and dissolve in aqueous leaf compartments thereby forming sulphurous acid, nitrous acid and nitric acid. Oxidative detoxification of SO_2 leads to the formation of sulfuric acid. Sulfate has been observed to accumulate in needles of spruce as a function of needle age [1] and the extent of air pollution with SO_2 [2]. Maximum levels were as high as 100 mM. This corresponds to a burden of 200 mM H^+ introduced from outside.

Normal metabolism involves many reactions that either produce or consume protons. Nitrogen is an important constituent of plant cells. The ammonium cation is usually taken up from the soil in exchange for a proton, whereas alkalization of the growth medium is observed when nitrate is absorbed by roots. Hydroxyl ions are liberated during nitrate reduction, whereas metabolization of ammonium ions liberates protons. Growth may dramatically depend on whether nitrate or ammonium are used as sources of nitrogen. Metabolic reactions involving consumption, production or transfer of protons must be seen in relation to the pH dependence of the activity of many enzymes. For instance, chloroplast sedoheptulose 1,7-bisphosphatase and fructose 1,6-bisphosphatase are highly sensitive to changes in pH [3]. In normal metabolism, such changes may be expected to be under metabolic control.

We were interested to know the extent to which leaves of pea plants, grown with either nitrate or ammonium salts, are capable of tolerating cytoplasmic acidification. Ammonium nutrition finally retards growth and results in premature ageing of pea plants which thrive when fertilized with nitrate. To induce acidification, we used either anaerobiosis or high concentrations of CO_2 . CO_2 dissolves in aqueous phases forming carbonic acid. pH values were measured *in vivo* by using ^{31}P -NMR [4].

2. Material and methods

2.1. Plants and growth conditions

Plants of *Pisum sativum* (pea) were grown either in vermiculite without added nitrogen-containing salts or in hydroponic culture with nitrate or ammonium salts as sole sources of nitrogen. In the presence of

nitrogen-containing salts, symbiotic nitrogen fixation is suppressed. Light intensity in the growth chamber used for growing the nitrogen-fertilized plants was about $250 \mu\text{mol} \cdot \text{m}^{-2} \cdot \text{s}^{-1}$ photosynthetically active radiation (PAR). Illumination was provided by HQI lamps (400 W, Schreder, Winterbach, Germany). Day length was 10 h, air temperature 23–24°C during the day and 16–17°C at night. The composition of the culture medium was (a) for nitrate plants: 1.5 mM $\text{Ca}(\text{NO}_3)_2$, 6 mM KH_2PO_4 , 2 mM KCl, 2 mM MgSO_4 , 2.5 mM CaSO_4 , 1 mM Fe-EDTA, and trace elements; b) for ammonium plants: 1.5 mM $(\text{NH}_4)_2\text{SO}_4$, 6 mM KH_2PO_4 , 1 mM CaCl_2 , 2 mM MgSO_4 , 1 mM CaSO_4 , 1 mM Fe-EDTA and trace elements. Eight plants were grown per pot which contained 1.8 l of aerated nutrient solution. The solution was replaced every third (young plants) or second (older plants) day. At the time of the harvest of leaves, fertilized plants had been on hydroponics for about 20 days. Unfertilized plants were used about two weeks after germination.

2.2. *In vivo* ^{31}P -NMR measurements

^{31}P -NMR spectra were recorded on a Bruker spectrometer (AMX 400, wide bore) tuned at 161.93 MHz. For a high signal to noise ratio, a 25 mm probe and a 25 mm flat bottom tube were used. Leaves were cut into strips, washed in water, suspended in 1 mM CaSO_4 and filled into the NMR tube above a porous polymer plate which was positioned near the bottom of the tube. The tube contained an inlet for perfusion medium which was introduced to the bottom of the tube and a safety exit which was positioned above the leaf material at the head of the NMR tube. A perfusion system adapted from the system described by [5] was used. A peristaltic pump circulated perfusion medium at a flow rate of 60 ml min^{-1} through the sedimented leaf material. Outside the spectrometer, it passed through a 4 liter reservoir which was bubbled either with air or oxygen (normoxia) or with nitrogen (anoxia). When desired, air used for aeration was replaced by a mixture of 85% air and 15% CO_2 , or a mixture of 85% nitrogen and 15% CO_2 . Gases were mixed with a Wösthoff pump (H. Wösthoff KG, Bochum, Germany). Unless stated otherwise, the perfusion medium contained 2 mM KNO_3 (for nitrate plants) or 2 mM $(\text{NH}_4)_2\text{SO}_4$

(for ammonium plants), 1 mM MgSO_4 , 1 mM CaSO_4 and 0.1 mM phosphate, pH 6.5. Where specified, 5 mM glucose and/or 5 mM mannose were also added. The pH of the circulating medium was controlled by a pH stat coupled to a titrimer (Uretron 6, Tacussel, France). The temperature of the perfusion medium was kept at 20°C. The amount of leaf material (9 to 10 g fresh weight) and incubation conditions were optimized. NMR spectra acquisition used 30- μs pulses (50°) at 0.6-s intervals. Free induction decays (FIDs) were recorded with 4K data points and zero-filled to 8K prior to Fourier transformation. Two levels of decoupling (Waltz pulse sequence) were used, 2.0 W during data acquisition (0.36 s) and 0.5 W during the delay period (0.24 s). Spectra are referenced to a solution of 50 mM methylenediphosphonic acid (MDP, pH 8.9 in 30 mM Tris, at 16.38 p.p.m.) in a 0.8 mm capillary which was inserted into the output tube along the symmetry axis of the NMR tube. The assignment of inorganic phosphate, phosphate esters and nucleotides to specific peaks was carried out according to Roberts and Jardetzky [6]. Spectra of perchloric acid extracts from the leaves were also used for reference purposes.

2.3. *In vitro* ^{31}P -NMR measurement

3 ml perchloric acid extract prepared from 9 g of pea leaves as described by Aubert et al. [7] were analyzed in a 10 mm NMR tube using a 10 mm probe, 15- μs pulses (70°) and 4.6-s intervals for spectra acquisition. The deuterium resonance of $^2\text{H}_2\text{O}$ was used as a lock signal. The spectra were recorded over a period of 1 h 20 min (1024 scans) at a sweep width of 6000 Hz under conditions of broad band proton decoupling with 8K data points zero-filled to 16K prior to Fourier transformation. Two levels of decoupling (Waltz pulse sequence) were used, 1.0 W during the data acquisition (1.24 s) and 0.25 W during the delay period (3.36 s). An exponential multiplication (0.2 Hz line width) was used to increase the signal to noise ratio. Spectra were referenced to methylenediphosphonic acid as described above. Before ^{31}P -NMR analysis, divalent cations were chelated by the addition of usually 60 μmol 1,2-cyclohexylenedinitrilotetraacetic acid. The pH of the samples was adjusted to 7.5 and buffered by the addition of 200 μmol Hepes.

2.4. Chlorophyll fluorescence

Modulated chlorophyll fluorescence emitted from small disks of pea leaves (4.15 cm^2), which were enclosed in a sandwich-type cuvette at 20°C, was measured with the PAM fluorometer of Walz, Effeltrich, Germany [8]. The gas phase was air or a mixture of air and CO_2 . Spikes of chlorophyll fluorescence were produced by saturating 1 second flashes of white light on top of stationary fluorescence which was elicited by background light (photon flux density, PFD, 500 or 1140 $\mu\text{mol} \cdot \text{m}^{-2} \cdot \text{s}^{-1}$). When divided by total fluorescence (stationary plus spike fluorescence), the spikes served to indicate the quantum efficiency of electron flow through photosystem II of the chloroplast electron transport chain [9].

2.5. Gas exchange

H_2O and CO_2 exchange of pea leaves were measured simultaneously with chlorophyll fluorescence using a conventional IRGA technique (IRGA, infrared gas analysis).

3. Results

3.1. Cytoplasmic acidification by CO_2

Fig. 1 shows typical ^{31}P -NMR signals from intact pea leaf tissue and from a pea leaf extract. When leaf strips were perfused in the NMR tube with aerated water in the presence of glucose, several resonance peaks representing phosphorylated intermediates populated the spectrum. Vacuolar phosphate was dominant, but sugar phosphates and nucleoside triphosphates were also clearly visible. Importantly, the smaller cytoplasmic phosphate peak and the much larger vacuolar phosphate peak were well separated. Increased resolution was achieved after perchloric acid extraction of the leaves permitting separation of component peaks into individual components (inset, upper lefthand side of Fig. 1).

The position of the phosphate peaks of the leaves relative to the p.p.m. scale at the abscissa is a function of pH of the cytoplasmic and vacuolar compartments. A calibration experiment is shown in Fig. 1 (inset, upper righthand side), where the position of

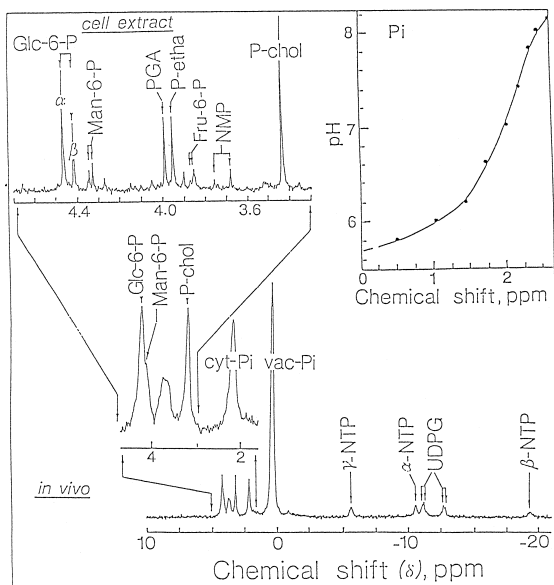


Fig. 1. Representative ^{31}P -NMR spectra of darkened pea leaf segments (lower spectra) and a pea leaf extract (upper lefthand side). The *in vivo* spectra were obtained with aerated leaf segments which were perfused with a medium containing 5 mM glucose. They are the result of 6000 transients (1 h). The inset in the upper righthand side of the figure shows the chemical shift of inorganic phosphate (P_i) versus pH, the inset in the upper lefthand side the upfield part of a spectrum obtained *in vitro* from a cell extract (1024 transients, 1 h 20 min). Pea plants were grown in vermiculite. Peak assignments: Glc-6-P, glucose 6-phosphate; Man-6-P, mannose 6-phosphate; Fru-6-P, fructose 6-phosphate; PGA, 3-phosphoglycerate; P-chol, phosphorylcholine; P-etha, phosphorylethanolamine; cyt- P_i , cytoplasmic phosphate (peak at 2.2 p.p.m. corresponding to P_i at pH 7.5; vac- P_i , vacuolar phosphate (peak at 0.35 p.p.m. corresponding to P_i at pH 5.8; UDPG, uridine 5'-diphosphoglucose; NMP, nucleoside monophosphates; α,β,γ -NTP: denotes phosphate positions in nucleoside triphosphates.

the phosphate peak is plotted against the pH of a leaf extract. If this calibration is used to determine pH values *in vivo*, then the cytoplasmic pH was about 7.5 and the vacuolar pH about 5.8 in the experiment of Fig. 1.

Perfusion of leaves in the absence of glucose decreased the peaks of the sugar phosphates. At much shorter time resolution than used for the experiments of Fig. 1, spectra were less detailed than shown, but phosphate peaks were always clearly resolved. Fig. 2 shows results of pH determinations in an experiment with ammonium-grown pea leaves. The time resolution is apparent from the data points. According to

the position of the phosphate peaks (p.p.m. scale), initial cytoplasmic and vacuolar pH values were about 7.6 and 5.6, respectively. Acidification by 15% CO_2 in air (about 5 mM in solution) shifted the phosphate peaks indicating decreased cytoplasmic and vacuolar pH values. Importantly, the kinetics of the decrease were remarkably different for the different compartments. In the cytoplasm, the maximum decrease in pH was reached after about 6 min and in the vacuoles after 15 min perfusion. In a similar experiment with nitrate-grown pea plants (not shown), the cytoplasmic pH decrease was somewhat faster than shown in Fig. 2 (maximum after 4 min) and the vacuolar decrease slower (20 min), but other results were similar.

It is important to note that the cytoplasmic pH decrease is much too fast to be explainable in terms of the uncatalyzed conversion of dissolved CO_2 into carbonic acid, which has a half time of about 30 s. Diffusion equilibrium between intercellular CO_2 and vacuolar CO_2 is reached within a fraction of a second. The contrasting kinetics of the cytoplasmic and vacuolar pH responses therefore show H^+ transport into the vacuoles. Indeed after the initial decrease, the

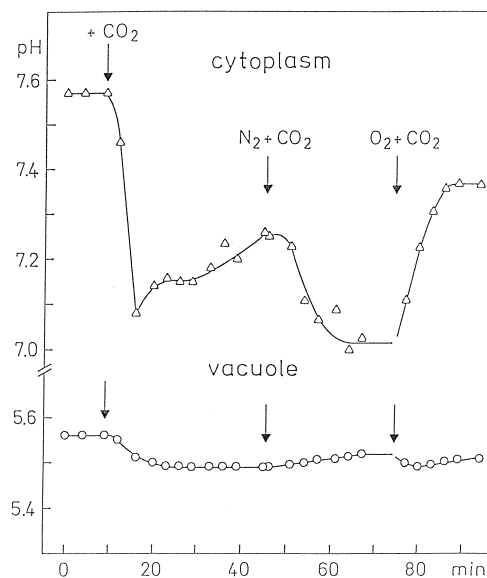


Fig. 2. Effects of acidification by CO_2 (15% in air), hypoxia and aeration on cytoplasmic and vacuolar pH values of leaves from pea plants which had been fertilized with ammonium. Acidification decreased and alkalization increased the position of ^{31}P NMP signals in the p.p.m. scale. This was used to determine pH (see inset in Fig. 1).

pH increased slowly in the cytoplasm in the presence of CO_2 .

When, still in the presence of high CO_2 , oxygen was replaced in the perfusion medium by nitrogen, the cytoplasmic pH decreased a second time after it had partially recovered from the initial CO_2 -dependent acidification. Whilst the cytoplasmic pH decreased under hypoxic conditions, the vacuolar pH increased suggesting efflux of protons from the vacuoles into the cytoplasm. This flux was reversed on returning to fully aerobic conditions. The final cytoplasmic pH reached in the experiment of Fig. 2 after about 80 min in the presence of high CO_2 was still about 0.2 pH units below the initial pH and the final vacuolar pH about 0.05 units below the initial pH. Different cytoplasmic and vacuolar buffering and different compartmental volumes explain the differences in the extent of cytoplasmic and vacuolar pH shifts which are indicated by the NMR data of Fig. 2.

3.2. Cytoplasmic acidification under anaerobiosis

In the experiment shown in Fig. 3, anaerobiosis was used instead of CO_2 to achieve cytoplasmic acidification and the leaf segments were perfused with either 5 mM glucose or 5 mM mannose. In contrast to mannose, glucose enters the glycolytic pathway after its phosphorylation. A distinct peak of glucose 6-phosphate is seen in NMR spectra only when glucose is present in the perfusion medium (Fig. 1). Obviously, glucose is readily taken up by the leaf segments. Mannose is known to sequester cytoplasmic phosphate by consuming ATP as it is phosphorylated by hexokinase [10,11]. Resulting mannose 6-phosphate is only slowly metabolized. Anaerobiosis caused the cytoplasmic pH to decrease from pH 7.5 to 6.5 both in the presence of glucose and of mannose. As the cytoplasmic pH decreased, the vacuolar pH increased.

Vacuolar alkalization under anaerobiosis is interpreted to indicate acid efflux from the vacuoles. The failure of the cytoplasm to respond by continued acidification to entering vacuolar acid after the pH had stabilized at pH 6.5 is thought to be caused in part by metabolic pH stabilizing reactions, i.e., by cytoplasmic base production or acid degradation, and in part by acid export from the cytoplasm into the apoplast [12].

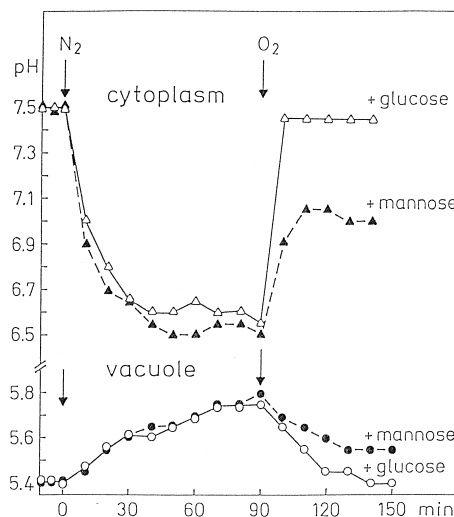


Fig. 3. Fig. 2. Effects of anaerobiosis and subsequent oxygenation on cytoplasmic and vacuolar pH values of pea leaves. Pea leaf segments in suspension were perfused with a medium containing either 5 mM glucose or 5 mM mannose. The medium was equilibrated either with oxygen or nitrogen. Acidification decreased and alkalization increased the position of ^{31}P NMP signals in the p.p.m. scale. This was used to determine pH (see inset in Fig. 1). Pea plants were grown in vermiculite.

After 90 min anaerobiosis, the perfusion medium was bubbled with oxygen. Oxygenation produced a rapid increase of the cytoplasmic pH and a slower decrease in the vacuolar pH. Apparently, acid was pumped from the cytoplasm into the vacuoles. The initial cytoplasmic pH was fully reestablished after about 10 min when glucose, but not, when mannose was present in the perfusion medium. In accordance with this, the vacuolar pH decreased to the level observed before anaerobiosis only in the presence of glucose, not with mannose.

3.3. Role of ATP in cytoplasmic pH regulation

Incomplete restoration of the initial cytoplasmic and vacuolar pH values after anaerobiosis in the presence of mannose suggests the involvement of ATP in the transport reactions which permit cytoplasmic pH restoration after a period of anaerobiosis. By consuming phosphate during its phosphorylation, mannose lowers ATP levels which are linked to phosphate levels through the phosphorylation potential $(\text{ATP})/((\text{ADP})(\text{P}_i))$. At constant phosphorylation potentials, the ratio of ATP to ADP must decrease when inorganic phosphate P_i decreases.

Fig. 4 compares ^{31}P -NMR spectra from aerobic (A) and anaerobic (B) leaf segments. The perfusion medium contained 5 mM glucose. In the presence of oxygen, the peak of glucose 6-phosphate was as prominent as the peak of cytoplasmic phosphate. The peaks of nucleoside triphosphates and of uridine diphosphoglucose were also clearly visible. Under anaerobiosis (anoxia), the peaks of glucose 6-phosphate, of the triphosphates and of uridine diphosphoglucose had all but disappeared. Obviously, anaero-

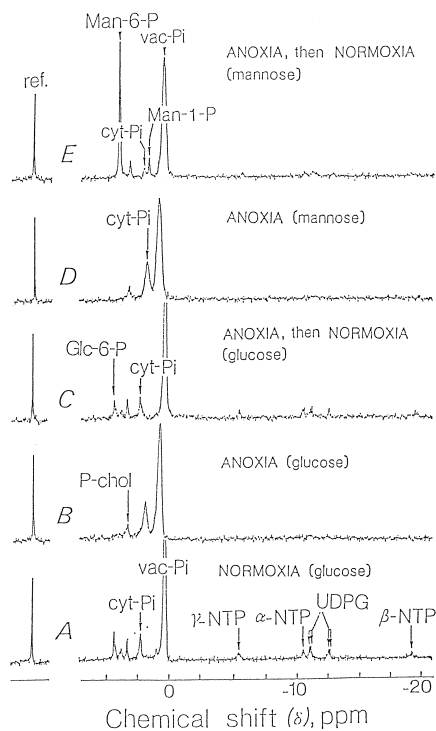


Fig. 4. Changes in the concentration and peak position of the most abundant P-compounds and inorganic phosphate in pea leaves perfused with a medium containing glucose after a change from normoxia (air, A) to anoxia (anaerobiosis, B) and then back to normoxia (C). In (D) and (E), mannose was supplied with the perfusion medium instead of glucose. Pea plants were grown in vermiculite. (A) Reference spectrum; (B) spectrum after 20 min anoxia; (C) after 30 min anoxia followed by 20 min reoxygenation; (D) after 20 min anoxia in the presence of 5 mM mannose; (E) after 30 min anoxia followed by 20 min reoxygenation in the presence of 5 mM mannose. For peak assignments, see legend to Fig. 1; in addition: Man-1-P, mannose 1-phosphate. It should be noted that anoxia and mannose narrowed the gap between the cytoplasmic and vacuolar phosphate peaks. By giving rise to the accumulation of mannosephosphates, mannose decreased the cytoplasmic concentrations of nucleoside triphosphates and inorganic phosphate even when oxygen was present.

biosis had drastically decreased the level of ATP. Simultaneously, the peak of vacuolar phosphate was decreased compared to the peak observed under aerobiosis, whereas the peak of cytoplasmic phosphate was increased in the absence of oxygen. The observations indicate efflux of phosphate from the vacuole into the cytoplasm. Also, the distance between the cytoplasmic and the vacuolar phosphate peaks had narrowed under anaerobiosis, with the cytoplasmic phosphate peak moving to the right and the vacuolar phosphate peak to the left. In agreement with the data shown in Fig. 3, this indicates cytoplasmic acidification and vacuolar alkalization.

The loss of ATP under anaerobiosis can be related to the efflux of protons and of phosphate from the vacuole. Indeed, oxygenation of leaf segments after a period of anaerobiosis led to the reappearance of the peaks of glucose 6-phosphate and of nucleoside triphosphates and widened the gap between the cytoplasmic and vacuolar phosphate peaks. Simultaneously, the vacuolar phosphate peak decreased and the vacuolar peak increased (Fig. 4C). As the cytoplasmic pH increased after oxygenation and the vacuolar pH decreased (Fig. 3), phosphate that had leaked into the cytoplasm under anaerobiosis was pumped back into the vacuole.

In Fig. 4D and E, a similar experiment is shown with mannose instead of glucose in the perfusion medium. The ^{31}P -NMR spectra seen with mannose and glucose under anaerobiosis were very similar. However, 20 min oxygenation after a 30 min period of anaerobiosis led to clear differences. In the presence of mannose, mannose 6-phosphate and mannose 1-phosphate accumulated. The peak of inorganic phosphate was much decreased. Whereas the peaks of nucleoside triphosphates were still discernible, they were clearly smaller than the peaks observed after anaerobiosis with glucose. The peak of vacuolar phosphate did not increase much after anaerobiosis and the gap between the cytoplasmic and vacuolar phosphate widened less under oxygenation than observed in the presence of glucose. These add to the findings shown in Fig. 3, where mannose, in contrast to glucose, did not permit full restoration of cytoplasmic and vacuolar pH values after a period of anaerobiosis. Apparently, mannose competed with the tonoplast ATPase for the ATP needed to pump protons and anions back into the vacuole from where they

had leaked into the cytoplasm which was largely deprived of ATP during anaerobiosis.

In Fig. 5, the time course of the accumulation of mannose 6-phosphate is shown in an experiment in which the perfusion medium was bubbled with 15% CO₂. Oxygen was present. In spectrum A, the perfusion medium contained neither glucose nor mannose. Glucose 6-phosphate was therefore largely absent. The spectra B, C and D were taken 13, 38 and 63 min after the introduction of mannose to the perfusion medium. The broad cytoplasmic phosphate peak decreased in the presence of mannose (Fig. 5B), shifted to the right indicating some acidification of the cytoplasm the pH of which was already lowered by the high CO₂ concentration, and then split into

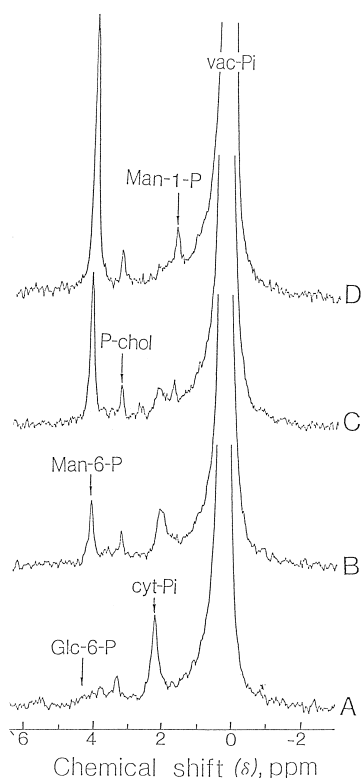


Fig. 5. ³¹P-NMR spectra of pea leaves. A: before addition of mannose to the perfusion medium. The peaks at 2.197 and 0.214 p.p.m. originate from cytoplasmic and vacuolar phosphate, respectively. B, C, D: 13, 38 and 63 min after addition of mannose to the perfusion medium. Note shifts in the position of the phosphate peaks. Glc-6-P, glucose 6-phosphate; Man-6-P, mannose 6-phosphate; Man-1-P, mannose 1-phosphate; P-chol, cholinphosphate; cyt-P_i, cytoplasmic phosphate; vac-P_i, vacuolar phosphate. Time resolution 15 min. The pea plants were grown with (NH₄)₂SO₄.

two components (Fig. 5C). The one to the left, inorganic phosphate, decreased and then almost disappeared as incubation with mannose was prolonged (Fig. 5D). The larger one was identified as mannose 1-phosphate. The shift in the phosphate peak seen in Fig. 5B and C relative to Fig. 5A then indicates that the cytoplasmic pH, which was already lowered in the presence of high CO₂, dropped further on addition of mannose to the perfusion medium. Simultaneously, the vacuolar pH increased indicating efflux of H⁺ from the vacuoles. The observations add to the data of Fig. 4 by showing that the sequestration of cytoplasmic phosphate by mannose is slow. In the experiment of Fig. 4 residual ATP is still available even in the presence of mannose to power the tonoplast ATPase sufficiently for considerable aerobic pH restoration.

It is also worth noting that the peak of mannose 6-phosphate continued to increase from (B) to (D) in Fig. 5. In (D) it was much larger than the cytoplasmic phosphate pool had been in (A). This shows also very clearly that mannose induced the release of phosphate from the vacuoles, most probably by lowering the cytoplasmic ATP level. ATP is needed to energize the tonoplast membrane and support the transtonoplast proton gradient.

Whereas the experiments involving anaerobiosis revealed rapid and full reversibility of pH changes after aeration, the initial acidic pH shift caused by high CO₂ was only slowly and incompletely replaced by a subsequent alkalization reaction (Fig. 2). The phosphate pools of the chloroplast stroma and the cytosol are known to be separated. However, since the NMR spectra of Fig. 1, Fig. 4 and Fig. 5 show only one cytoplasmic phosphate peak, the pH values of chloroplast stroma and cytosol must have been similar. Because no splitting of the cytoplasmic phosphate peak was observed after the addition of high CO₂, the acidic pH shift produced by CO₂ was also similar in the chloroplast stroma and the cytosol. This has consequences for chloroplast performance as shown below.

3.4. Response of photosynthesis to cytoplasmic acidification

Photosynthesis is known to be sensitive to a lowering of the pH of the chloroplast stroma [13]. Linear

electron flow in photosynthesis can be deduced from simple measurements of modulated chlorophyll fluorescence [9], whereas carbon assimilation can be measured by infrared gas analysis. In Fig. 6, simultaneous recordings of modulated chlorophyll fluorescence (A) and of IRGA measurements (B) are shown for a leaf of an ammonium-fertilized pea plant. Total electron flow was calculated from the fluorescence data [9].

When a modulated measuring beam of extremely low intensity was turned on in the absence of actinic illumination, modulated fluorescence from the leaf rose to the low level F_0 . In the beginning of the

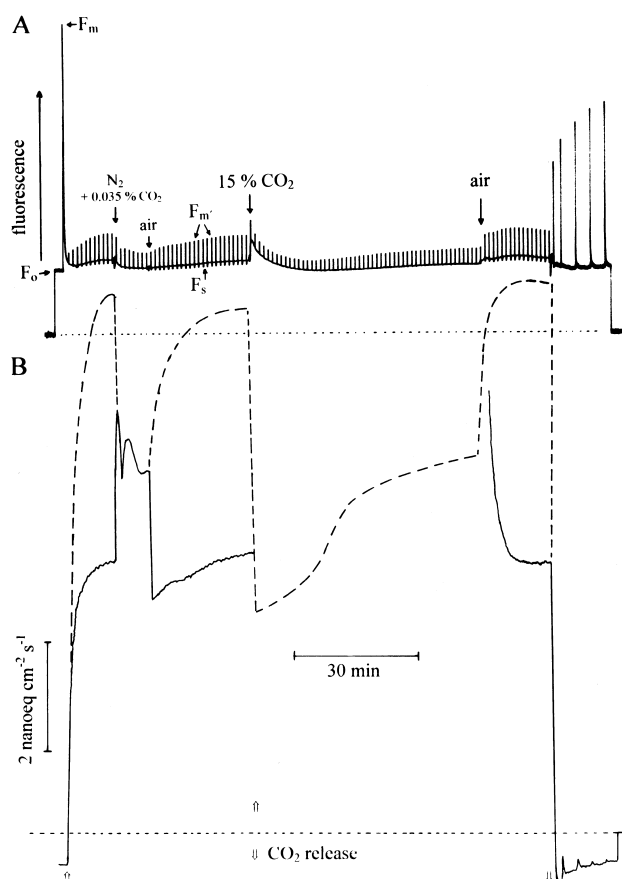


Fig. 6. Modulated chlorophyll fluorescence (A), total calculated electron transport (dashed line) and measured electron transport to external CO_2 in air or nitrogen with 350 p.p.m. CO_2 (B) of a leaf from an ammonium-fertilized pea plant. 15% CO_2 were added to or removed from air as indicated. Illumination with $PFD = 1140 \mu mol \cdot m^{-2} \cdot s^{-1}$. Every 60 s a strong light pulse ($PFD > 4000 \mu mol \cdot m^{-2} \cdot s^{-1}$) lasting 1 s was given. For an explanation, see text.

experiment, the darkened leaf was kept in air. On turning actinic light on (photon flux density, $PFD = 1140 \mu mol \cdot m^{-2} \cdot s^{-1}$), fluorescence increased to the transient maximum F_m and then declined rapidly in the so-called Kautsky effect [15–17] towards low levels which may be designated F_s . 1-s pulses of saturating light ($PFD > 4000 \mu mol \cdot m^{-2} \cdot s^{-1}$) given on top of actinic illumination produced fluorescence spikes which at maximum are designated F_m' . They were small at first, increased towards a steady state, decreased under nitrogen, increased again in air and became small in the presence of 15% CO_2 in air. While exposure of the leaf to 15% CO_2 continued, the spikes increased slowly. They increased rapidly, as high CO_2 was replaced by air. After darkening, the spikes became very large.

Since the ratio of the spikes to total fluorescence $(F_m' - F_s)/F_m'$ is a measure of the quantum efficiency $\Phi_{PS II}$ of electron flow through PS II [9], increasing spike height in the presence of actinic light indicates increased electron flow through photosystem II. Main reactions supporting electron flow through photosystem II are carbon assimilation and oxygen reduction during photorespiration and the Mehler reaction. However, only carbon assimilation can proceed in the absence of oxygen. The very low concentration of oxygen generated during carbon assimilation in nitrogen does not support measurable oxygen reduction. Thus, carbon assimilation measured by IRGA in nitrogen (see lower part of Fig. 6) can be used to calibrate the electron flow through photosystem II which is indicated by the fluorescence data $(F_m' - F_s)/F_m'$. The dashed line in the lower part of Fig. 6 indicates total electron transport. In air, it was almost twice as large as assimilatory electron transport to external CO_2 . In nitrogen, total electron transport and assimilatory electron transport coincided. In 15% CO_2 , carbon uptake could not be measured by the IRGA technique, but total electron transport could be calculated. It is likely to be identical with assimilatory electron transport because photorespiration is known to be suppressed in high CO_2 . The fluorescence data indicate a strong depression of total electron transport. Significantly, electron transport increased during the continuing presence of 15% CO_2 . This slow increase is impressively similar to the slow increase in cytoplasmic pH seen in the presence of 15% CO_2 (Fig. 2). Apparently, cytoplas-

mic pH regulation extended to the chloroplasts and resulted in the partial recovery of photosynthetic electron transport which had been inhibited by acidification of the chloroplasts stroma. It is noteworthy that high CO_2 failed to result in stomatal closure. This is apparent from transpiration data (not shown, but H_2O exchange was recorded together with CO_2 exchange) and from persisting carbon assimilation after the CO_2 concentration in air was decreased from 15% to 0.035% (Fig. 6).

In Fig. 7, the relative quantum efficiency of electron transport $\Phi_{\text{PS II}} = (F_m' - F_s)/F_m'$ is shown as a function of time of exposure pea leaves to different CO_2 concentrations. As in Fig. 6, the leaves were from an ammonium-fertilized plant. However, in contrast to the experiment shown in Fig. 6, they had been briefly exposed to high CO_2 in the dark before they were illuminated. Whereas illumination in air (Fig. 6) resulted in fast CO_2 uptake, light-driven electron transport in the presence of high CO_2 (Fig. 6 and Fig. 7) increased only slowly. Recovery of high rates of

electron transport was faster in 7% CO_2 , than in 15% or 25% CO_2 . It is important to note that electron transport per se was not inhibited by high CO_2 . This is seen as a result of the first two 1-s light pulses in the absence of stationary actinic illumination (inset of Fig. 7), where $(F_m - F_0)/F_m$ was close to 0.8, indicating a high quantum efficiency of electron flow through photosystem II [14] in all leaves irrespective of CO_2 concentration. Thus, inhibition of photosynthesis by high CO_2 is not due to inhibition of electron flow within the electron transport chain, but rather to inhibition of pH-sensitive enzymes of the photosynthetic carbon cycle.

3.5. pH regulation in relation to the nitrogen nutrition of pea plants

Experiments similar to those shown in Fig. 6 and Fig. 7 were also performed with leaves from nitrate-grown pea plants. Essentially similar results were usually obtained, but leaves from plants which had

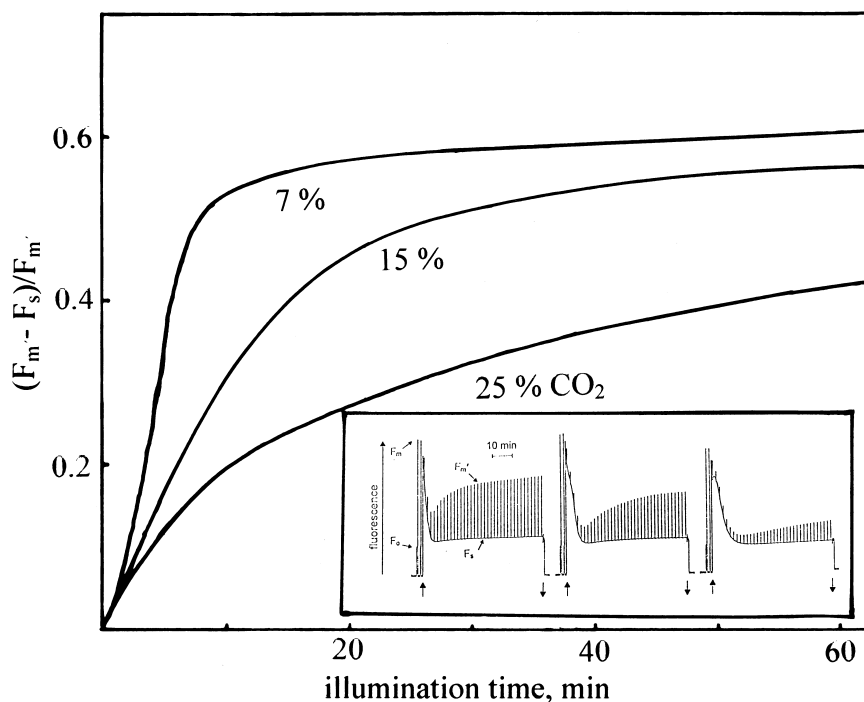


Fig. 7. Relative quantum efficiencies of electron transport through Photosystem II of leaves from an ammonium-fertilized pea plant as a function of exposure time to high CO_2 in air. Darkened leaves were exposed to 7, 15 or 25% CO_2 and then illuminated with $\text{PFD} = 500 \mu\text{mol} \cdot \text{m}^{-2} \cdot \text{s}^{-1}$. Since light was constant, quantum efficiencies are directly proportional to rates of electron transport. The inset shows the recordings of modulated chlorophyll fluorescence from which quantum efficiencies were calculated. Every 100 s a strong light pulse ($\text{PFD} > 8000 \mu\text{mol} \cdot \text{m}^{-2} \cdot \text{s}^{-1}$) lasting 1 s was given. For further explanation, see text.

been grown with ammonium as nitrogen source appeared to be slightly more, not less, tolerant to high CO_2 than leaves from nitrate-grown plants even though growth of ammonium-grown plants was reduced after three weeks exposure to ammonium nutrition and the leaves contained less chlorophyll than leaves of nitrate-grown plants. Apparently, ammonium nutrition does not affect the ability of leaves to counter CO_2 -dependent acidification by pH regulation. For this reason, retarded growth cannot be attributed to ineffective pH regulation in ammonium-fertilized pea plants.

4. Discussion

CO_2 readily diffuses across biomembranes. Its pK is 6.37 in water at room temperature and may be as low as 6.1 at the ionic strength of cellular compartments [18]. The solubility in water is given by the Bunsen coefficient as 0.82 cm^{-1} at 20°C . This means that in the NMR experiments 15% CO_2 in air equilibrate with 5.1 mM CO_2 in aqueous solution, whereas in the fluorescence experiments 7, 15 and 25% CO_2 (Fig. 7) equilibrate with 2.4, 5.1 and 8.5 mM CO_2 in aqueous cellular compartments. In solution, CO_2 consumes OH^- during its conversion to HCO_3^- . In the chloroplasts of pea leaves this consumption is rapid because of the presence of carbonic anhydrase. In the vacuoles, it is slow (half time of the uncatalyzed reaction 30 s at 20°C [19].

The relationship between the concentration of dissolved CO_2 and the accumulation of bicarbonate (i.e., the consumption of OH^-) at different pH values is given by the Henderson/Hasselbalch equation as

$$\text{pH} = pK + \log \left(\frac{[\text{HCO}_3^-]}{[\text{CO}_2]} \right)$$

Obviously, the extent of a passive decrease in pH of a cellular compartment caused by a constant concentration of 5.1 CO_2 in solution depends on the initial pH of that compartment and on the buffering capacity of its solutes. Thus, if the initial pH of the cytoplasm of pea leaves is assumed to be 7.5 and the CO_2 concentration is 5.1 mM, the cytoplasmic pH should in the absence of metabolic pH control be expected to drop to about 6.8, if the buffering capacity is 35 mM/pH unit, or to 6.95, if the buffering capacity is as high as 70 mM/pH unit. Buffering capacities of about 35

mM/pH unit have been reported for aqueously isolated chloroplasts and chloroplasts in situ [20,21] but higher buffer capacities were obtained by titration of non-aqueously isolated chloroplasts [22].

The observed maximum cytoplasmic decrease in pH on addition of 15% CO_2 in air (5.1 mM CO_2 in solution) was close to 0.5 pH units (Fig. 2), not far from the 0.55 pH units expected from a buffering capacity of 70 mM/pH unit. While the cytoplasmic pH recovered partially after its initial fast decrease, the vacuolar pH continued to decrease suggesting the transfer of protons from the cytoplasm into the vacuoles [12,23]. According to the Henderson/Hasselbalch equation, an increase in cytoplasmic pH must at constant CO_2 be accompanied by an increase in cytoplasmic bicarbonate. This increase needs cations as counterions to bicarbonate. In the experiment of Fig. 2, 17 mM bicarbonate accumulated after 35 min aerobic acid stress and 46 mM after 80 min including a period of hypoxia. Obviously, a corresponding concentration of cations had to become available to permit this accumulation. Either there is proton/cation exchange across the tonoplast or anions leave the cytoplasm together with protons. In both cases proton transport has to be energized because the vacuolar pH is lower than the cytoplasmic pH. Energization of proton export is shown by the effects of hypoxia and subsequent aeration (Fig. 2) and by the acidifying effect mannose has on the cytoplasm in the presence of CO_2 and oxygen (Fig. 5C). The tonoplast contains two proton-translocating enzymes, an ATPase and a pyrophosphatase. As hexokinase uses ATP, the cytoplasmic acidification and the vacuolar alkalization observed in the presence of mannose show that the tonoplast ATPase is active in cytoplasmic pH regulation. Almost nothing is known about the regulation of the tonoplast ATPase. The observations show that this membrane enzyme senses pH and is activated in vivo by cytosolic acidification.

Cytoplasmic pH regulation in the presence of high CO_2 occurs not only at the level of the cytosol and the vacuole. Chloroplasts are bounded by two membranes. The inner membrane of chloroplasts has a low principal permeability for protons, cations and anions, but contains regulated ion channels [24,25]. The most plausible explanation for the slow activation of photosynthesis under acid stress, which is shown in Fig. 6 and Fig. 7, is that photosynthesis

becomes possible only as the stromal pH is increased after its initial CO₂-dependent decrease during trans-envelope proton/cation exchange or proton/anion cotransport. In recent experiments involving non-aqueous chloroplast isolation, evidence favoring pH regulation by proton/anion export from the chloroplasts was obtained after leaves had been exposed to high CO₂ [22].

There is the question whether pH regulation after a period of anaerobiosis is different from the pH regulation observed under CO₂-dependent acidification. In the absence of oxygen, the cytoplasmic pH decreased and the vacuolar pH increased (Fig. 3), whereas in the presence of high CO₂, both cytoplasmic and vacuolar pH values decreased. In the case of anaerobiosis, protons and anions entered the cytoplasm. For phosphate this is shown in Fig. 4. Aeration rapidly restored the pH values observed before anaerobiosis (Fig. 3). This fast restoration did not occur on the basis of cation/proton exchange. Rather, phosphate followed the protons when these were pumped back into the vacuole. pH regulation appeared to involve mainly proton/anion cotransport. The tonoplast ATPase was the driving force for pH restoration. This is shown by the effects of mannose in Fig. 3 and Fig. 4. While sequestering phosphate (Fig. 5), mannose decreased cytoplasmic ATP levels making ATP less available for ion pumping across the tonoplast. This explains the ineffectiveness of pH restoration in the presence of mannose.

In NMR or photosynthesis experiments involving leaves either from pea plants fertilized with nitrate or with ammonium salts, no principal differences in the sensitivity to acidification or in pH regulation was observed. The reduced growth of plants often observed under ammonium nutrition may be explained by interference between the uptake of ammonium and other cations through the root system (i.e., by cation competition) rather than by increased cellular acidification [26].

In acid stress experiments with plant cells in suspension culture [12], the plasma membrane ATPase appeared to be mainly involved in countering cytoplasmic acidification. The present experiments suggest a main involvement of the tonoplast ATPase in leaves. Leaves are limited in their capacity for proton/cation exchange between cytoplasm and the external medium or for proton/anion export to the

apoplast. The limited apoplastic space of intact leaves is, in contrast to the large vacuoles inside differentiated cells, neither a suitable reservoir for protons and anions nor can it export as many cations into the cytoplasm as required under severe CO₂-dependent acid stress.

References

- [1] W. Kaiser, A. Ditttrich, U. Heber, *Tree Physiol.* 12 (1993) 1–13.
- [2] Slovik, S., Siegmund, A., Führer, H.-W. and Heber, U. (1995) *New Phytol.*, in press.
- [3] D. Baier, E. Latzko, *Biochim. Biophys. Acta* 396 (1975) 141–148.
- [4] R. Bligny, P. Gardestroem, C. Roby, R. Douce, *J. Biol. Chem.* 265 (1990) 1319–1326.
- [5] C. Roby, J.-B. Martin, R. Bligny, R. Douce, *J. Biol. Chem.* 262 (1987) 5000–5007.
- [6] J.K.M. Roberts, O. Jardetzky, *Biochim. Biophys. Acta* 639 (1981) 53–76.
- [7] S. Aubert, E. Gout, R. Bligny, R. Douce, *J. Biol. Chem.* 269 (1994) 21420–21427.
- [8] U. Schreiber, U. Schliwa, W. Bilger, *Photosynth. Res.* 10 (1986) 51–62.
- [9] B. Genty, J.-M. Briantais, N.R. Baker, *Biochim. Biophys. Acta* 990 (1989) 87–92.
- [10] Chen-She Sheu-Hwa, Lewis, D.H. and Walker, D.A. (1975) *New Phytol.* 74, 383–392.
- [11] C. Foyer, D.A. Walker, C. Spencer, B. Mann, *Biochem. J.* 202 (1981) 429–434.
- [12] E. Gout, R. Bligny, R. Douce, *J. Biol. Chem.* 267 (1992) 13903–13909.
- [13] K. Werdan, H.W. Heldt, M. Milovancev, *Biochim. Biophys. Acta* 396 (1975) 276–292.
- [14] O. Björkman, B. Demmig, *Planta* 170 (1987) 489–504.
- [15] H. Kautsky, A. Hirsch, *Naturwiss.* 19 (1931) 964.
- [16] G.H. Krause, *Biochim. Biophys. Acta* 292 (1973) 715–728.
- [17] G.H. Krause, E. Weis, *Ann. Rev. Plant Physiol. Plant Mol. Biol.* 42 (1991) 313–349.
- [18] A. Yokota, S. Kitaoka, *Biochem. Biophys. Res. Commun.* 131 (1985) 1075–1079.
- [19] G.S. Espie, B. Colman, *Plant Physiol.* 80 (1986) 863–869.
- [20] H. Pfanz, U. Heber, *Plant Physiol.* 81 (1986) 597–602.
- [21] M. Hauser, H. Eichelmann, U. Heber, A. Laisk, *Planta* 196 (1995) 199–204.
- [22] Hauser, M. (1996) Doctoral Dissertation, University of Würzburg.
- [23] U. Heber, U. Wagner, W. Kaiser, S. Neimanis, K. Bailey, D. Walker, *Plant Cell Physiol.* 34 (1994) 479–488.
- [24] W. Wu, G.A. Berkowitz, *Plant Physiol.* 98 (1992) 666–672.
- [25] I. Pottosin, *FEBS Lett.* 308 (1992) 87–90.
- [26] B. Lang, W.M. Kaiser, *New Phytol.* 128 (1994) 451–459.